
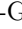










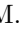











Gamma decay of the ^{154}Sm Isovector Giant Dipole Resonance: Smekal-Raman Scattering as a Novel Probe of Nuclear Ground-State Deformation

J. Kleemann ^{1,*} N. Pietralla ¹ U. Friman-Gayer ^{2,3,†} J. Isaak ¹ O. Papst ¹ K. Prifti ¹ V. Werner ¹ A. D. Ayangeakaa ^{4,3} T. Beck ^{1,‡} G. Cold ⁵ M. L. Cortés ¹ S. W. Finch ^{2,3} M. Fulghieri ^{4,3} D. Gribble ^{4,3} K. E. Ide ¹ X. K.-H. James ^{4,3} R. V. F. Janssens ^{4,3} S. R. Johnson ^{4,3} P. Koseoglou ¹ Krishichayan ^{2,3} D. Savran ⁶ and W. Tornow ^{2,3}

¹*Technische Universität Darmstadt, Department of Physics, Institute for Nuclear Physics, 64289 Darmstadt, Germany*

²*Department of Physics, Duke University, Durham, North Carolina 27708-0308, USA*

³*Triangle Universities Nuclear Laboratory, Duke University, Durham, North Carolina 27708, USA*

⁴*Department of Physics and Astronomy, University of North Carolina at Chapel Hill, North Carolina 27599-3255, USA*

⁵*Dipartimento di Fisica, Università degli Studi di Milano and Istituto Nazionale di Fisica Nucleare, Sezione di Milano, 20133 Milano, Italy*

⁶*GSI Helmholtzzentrum für Schwerionenforschung GmbH, 64291 Darmstadt, Germany*

(Dated: July 1, 2024)

The γ decays of the Isovector Giant Dipole Resonance (GDR) of the deformed nucleus ^{154}Sm from 2_1^+ -Smekal-Raman and elastic scattering were measured using linearly polarized, quasi-monochromatic photon beams. The two scattering processes were disentangled through their distinct angular distributions. Their branching ratio and cross sections were determined at six excitation energies covering the ^{154}Sm GDR. Both agree with the predictions of the geometrical model for the GDR and establish γ decay as an observable sensitive to the structure of the resonance. Consequently, the data place strong constraints on the nuclear shape, including the degree of triaxiality. The derived ^{154}Sm shape parameters $\beta = 0.2926(26)$ and $\gamma = 5.0(14)^\circ$ agree well with other measurements and recent Monte Carlo Shell-Model calculations.

The nuclear Isovector Giant Dipole Resonance (GDR) is a fundamental mode of excitation inherent to all nuclei [1, 2]. It dominates their photonuclear responses as it exhausts most [1, 3] of the appropriate sum rule for the electric dipole strength; i.e. the Thomas-Reiche-Kuhn sum rule [4, 5] multiplied by $(1 + \kappa)$, where κ is the enhancement factor [6]. Since its discovery in the early days of nuclear physics [7–9], the GDR as a ground-state excitation has continuously attracted a great deal of attention [1, 3, 6, 10, 11]. It has also been investigated as a function of temperature [12–15] and analogues to the nuclear GDR were identified in other multiparticle systems such as atoms [16–21], metallic clusters [22–24], and fullerenes [25, 26]. In the geometrical macroscopic liquid-drop model, the nuclear GDR is considered to be a collective isovector oscillation of the protons against the neutrons [27, 28] while, microscopically, it is understood as a collective coherent one-particle-one-hole excitation of the ground state [6, 29]. Its excitation energy ranges between 10 and 25 MeV, depending on the mass number. The GDR is, hence, particle unbound and decays predominantly by neutron emission, but also with a probability of about 1% by internal γ decay [30, 31].

As a ground-state excitation, the GDR is sensitive to ground-state properties, especially the nuclear shape. In spherical nuclei its photoabsorption cross section typically has a Lorentzian shape with a width of a few MeV, while in heavy, deformed nuclei a splitting into two overlapping Lorentzians is observed [1]. This phenomenon is considered to be one of the prime signatures of nuclear

deformation and is understood through the axial deformation allowing vibrations of protons against neutrons parallel or perpendicular to the nuclear symmetry axis with differing frequencies [32, 33]. The two oscillation modes are commonly assigned K quantum numbers of $K = 0$ for the parallel and $K = 1$ for the perpendicular vibration, respectively [3]. This geometrical picture is widely accepted in textbooks [3] due to its appealing simplicity. The GDR's photoabsorption cross section has been studied extensively in photoabsorption and particle-scattering reactions for many nuclei [1, 2]. At the same time, this macroscopic interpretation has consequences for the γ decay of the GDR, especially for the branching ratio of photon scattering reactions to the ground state and to the 2_1^+ member of the ground-state rotational band [34–36]. The latter may be addressed as a Smekal-Raman scattering (SRS) process. However, the GDR's γ decay, a fundamental property associated with its internal structure, was never studied systematically. Only few measurements exist, which lack either multiple excitation energies [35–37] or sufficient resolution and statistics [38–40]. Hence, a close experimental assessment of the geometrical model of the GDR in deformed nuclei in terms of its prediction of the γ -decay behavior was never performed thus far.

It is the purpose of this letter to report on the first systematic, energy-resolved study of the evolution of the γ -decay behavior of the GDR in a deformed nucleus, ^{154}Sm used here as an example, and to discuss its implications.

Nuclear Resonance Fluorescence (NRF) experi-

ments [34, 41–44] on the GDR of ^{154}Sm have been performed at the High-Intensity γ -ray Source (HI γ S) [45, 46] located at the Triangle Universities Nuclear Laboratory. By irradiating a $2.42(8)\text{ g/cm}^2$ Sm_2O_3 target enriched to $98.5(1)\%$ in ^{154}Sm with polarized, quasi-monochromatic γ -ray beams provided by HI γ S, around 0.3 MeV wide slices of the ^{154}Sm GDR were photo-excited. With a probability of about 1% , the GDR promptly decayed internally via the emission of photons. The latter were detected by four $3'' \times 3''$ LaBr_3 and four HPGe clover detectors of the Clover Array setup [47] arranged in a close geometry around the target. The LaBr_3 detectors were mounted at a polar angle of $\theta = 90^\circ$ with respect to the beam direction and azimuthal angles of $\phi \in \{0^\circ, 90^\circ, 180^\circ, 270^\circ\}$ with respect to the polarization plane, while the clover detectors were placed at $\theta \in \{125^\circ, 135^\circ\}$ and $\phi \in \{45^\circ, 180^\circ, 225^\circ, 315^\circ\}$. Data were taken at beam energies, E_{Beam} , of $11.37, 12.59, 14.27, 15.35, 16.16$ and 17.79 MeV , chosen to cover the ^{154}Sm GDR. The photon beams had slightly asymmetric Gaussian shapes $P(E)$ with bandwidths of $\text{FWHM}/E_{\text{Beam}} \approx 2\%$. The γ signals from elastic scattering (ES) and 2_1^+ -SRS on the GDR both share the shape of the beam profile $P(E)$ since within the narrow energy bandwidths of the beams the cross sections can be considered constant. In the case of 2_1^+ -SRS, this peak is additionally shifted down in energy by its excitation energy; i.e. $E_{2_1^+} = 0.082\text{ MeV}$ [48] for ^{154}Sm . Since this shift is smaller than the beam bandwidths, the two signals overlap and cannot be energy-resolved in the individual spectra. However, when exciting the $J^\pi = 1^-$ GDR of even-even nuclei with a linearly polarized photon beam, and assuming a pure electric dipole decay to the 2_1^+ state, the angular distributions

$$W_{0^+ \rightarrow 1^- \rightarrow 0^+}^{(\text{ES})}(\theta, \phi) = \frac{3}{4}(1 + \cos^2 \theta - \sin^2 \theta \cos 2\phi) \quad (1)$$

and

$$W_{0^+ \rightarrow 1^- \rightarrow 2^+}^{(2_1^+ \text{-SRS})}(\theta, \phi) = \frac{3}{40}(13 + \cos^2 \theta - \sin^2 \theta \cos 2\phi) \quad (2)$$

of these scattering processes [49–52] differ significantly at $\theta = 90^\circ$. Hence, the scattering intensities can be extracted from the observed azimuthal asymmetries of the doublet peaks. The detector response \mathcal{R} , due mostly to escape peaks and the Compton continuum, was taken into account in the analysis, since, at energies $> 10\text{ MeV}$, it dominates the spectra. Simulations of the responses were performed using GEANT4 [53–56], taking into account the full experimental setup and the known angular distributions of the observed radiations. For the analysis of the spectra, first the overall expected radiation was modeled as a sum of two asymmetric Gaussian peaks of the same shape $P(E)$, but different intensities I and shifted by 0.082 MeV with respect to each other on a small background \mathcal{B} . By convolving each part of

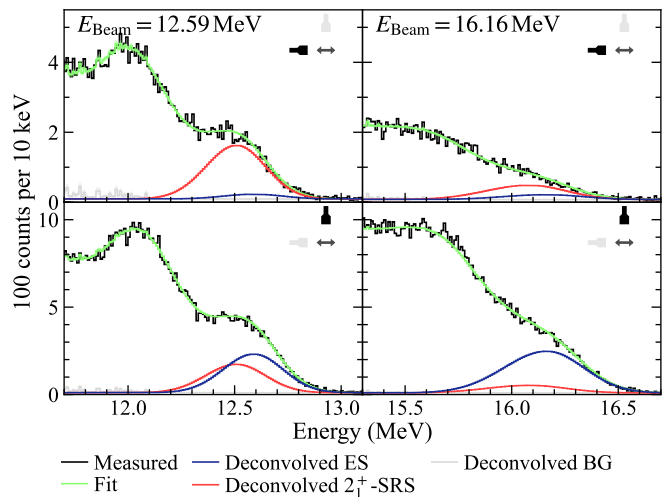


FIG. 1. Histograms (black) of the ^{154}Sm GDR γ decay at 12.59 MeV (left) and 16.16 MeV (right) excitation energy measured by LaBr_3 detectors in (top) and perpendicular to (bottom) the beam polarization plane along with the fitted spectra (green). The three components (“Deconvolved”) of the fit before convolution with the detector responses are shown as well, scaled to the full energy peak efficiencies of the detectors, i.e., as response-less detectors would have measured them. The background (BG) component is barely visible. The ES and 2_1^+ -SRS intensities are effectively obtained from the fitted azimuthal asymmetries of the spectra. Since the azimuthal asymmetry (top vs bottom) at 12.59 MeV is lower than at 16.16 MeV , its $\sigma_{2_1^+}/\sigma_{\text{ES}}$ branching ratio is higher.

this model with its corresponding simulated detector response, which includes the angular distribution effects and detector efficiencies, a fit-spectrum

$$\begin{aligned} \mathcal{S}^d(E) = & I_{2_1^+} \mathcal{R}_{2_1^+}^d * P(E + E_{2_1^+}) \\ & + I_{\text{ES}} \mathcal{R}_{\text{ES}}^d * P(E) + \mathcal{R}_{\mathcal{B}}^d * \mathcal{B}(E) \end{aligned} \quad (3)$$

is obtained for every detector d . By simultaneously fitting Eq. (3) to all 8 observed spectra in a global Bayesian inference Markov chain Monte Carlo approach [57–60], the intensities I_x of ES and 2_1^+ -SRS on the ^{154}Sm GDR were extracted from the azimuthal asymmetries and, therefore, also the branching ratio $\sigma_{2_1^+}/\sigma_{\text{ES}} = I_{2_1^+}/I_{\text{ES}}$. Figure 1 presents the observed ^{154}Sm GDR γ -decay spectra of the $\phi \in \{180^\circ, 90^\circ\}$ LaBr_3 detectors at $E_{\text{Beam}} \in \{12.59\text{ MeV}, 16.16\text{ MeV}\}$ along with the fitted spectra for the determination of the transitions’ intensities. The reliability of the method was confirmed through the analysis of calibration spectra taken with linearly and circularly polarized γ beams on ^{140}Ce at every beam energy, on ^{12}C at 15.35 MeV , and on ^{28}Si at 11.37 MeV . ^{12}C and ^{28}Si each caused one well-defined NRF peak from strong isolated $J^\pi = 1^+$ resonances [61, 62], while for ^{140}Ce the ES on the GDR is well-isolated, due to the high excitation energy of its first excited state at $E_{2_1^+} = 1.6\text{ MeV}$ [63]. Finally, absolute photon scattering

TABLE I. Results of the spectra analysis. E denotes the centroid energy of the γ beam with which the GDR was photoexcited and FWHM its full width at half maximum.

E_{Beam} (MeV)	FWHM (MeV)	$\sigma_{2_1^+}/\sigma_{\text{ES}}$	σ_{ES} (mb)	$\sigma_{2_1^+}$ (mb)
11.37(1)	0.33(1)	0.978(23)	0.70(9)	0.69(8)
12.59(1)	0.27(3)	1.017(15)	1.49(14)	1.52(15)
14.27(1)	0.28(1)	0.878(17)	1.61(15)	1.41(13)
15.35(1)	0.34(1)	0.436(34)	2.80(27)	1.22(14)
16.16(1)	0.32(1)	0.2550(43)	3.01(29)	0.77(8)
17.79(1)	0.41(1)	0.0964(32)	2.24(27)	0.216(27)

cross sections σ_{ES} for ES and $\sigma_{2_1^+}$ for 2_1^+ -SRS were determined, as well. This was achieved through simultaneous irradiation of thin ^{197}Au and $^{\text{nat}}\text{CeO}_2$ targets by the γ beam during the experiment and subsequent determination of their activation, due to (γ, n) reactions, which enabled the calibration of the photon fluxes relative to the known $^{197}\text{Au}(\gamma, n)^{196}\text{Au}$ and $^{140}\text{Ce}(\gamma, n)^{139}\text{Ce}$ cross sections [64, 65]. Table I provides our primary results.

The $\sigma_{2_1^+}/\sigma_{\text{ES}}$ γ -decay branching ratios were interpreted through scattering theory using the geometrical model of the GDR. Since NRF on the GDR to the 0_1^+ state is indistinguishable from Thomson scattering (ES of photons off the nucleus as a whole), these processes interfere with each other [34–36]. Hence, the total ES cross section is

$$\sigma_{\text{ES}}(E) = \frac{8\pi}{3} |f_{\text{GDR}}(E) + f_{\text{T}}|^2, \quad (4)$$

where the $f \in \mathbb{C}$ are the forward ($\theta = 0$) GDR 0_1^+ NRF and Thomson scattering amplitudes, respectively. As both scattering processes share the angular distribution of Eq. (1), this was factored out and integrated over the full solid angle. The Thomson amplitude $f_{\text{T}} = -Z^2 e^2 / (4\pi\epsilon_0 M c^2)$ for forward scattering on a nucleus of charge Ze and mass M is well-known, real and energy-independent [34], while the GDR 0_1^+ NRF amplitude $f_{\text{GDR}}(E)$ can be obtained from its total photoabsorption cross section $\sigma_{\text{abs}}(E)$ using the optical theorem and the dispersion relations [66] as

$$f_{\text{GDR}}(E) = \frac{E^2}{2\pi^2 \hbar c} \underbrace{\mathcal{P} \int_0^\infty \frac{\sigma_{\text{abs}}(\epsilon)}{\epsilon^2 - E^2} d\epsilon}_{\text{Cauchy principal value integral}} + i \frac{E\sigma_{\text{abs}}(E)}{4\pi \hbar c} \quad (5)$$

$$= \sum_{k=1}^3 \underbrace{\frac{\sigma_{0k} E^2 \Gamma_k}{4\pi \hbar c} \frac{(E_{0k}^2 - E^2) + iE\Gamma_k}{(E_{0k}^2 - E^2)^2 + E^2 \Gamma_k^2}}_{f_{\text{GDR}_k}(E)} \quad (6)$$

using the standard Lorentzian (SLO) parametrization of the GDR's photoabsorption cross section

$$\sigma_{\text{abs}}(E) = \sum_{k=1}^3 \frac{\sigma_{0k} E^2 \Gamma_k^2}{(E_{0k}^2 - E^2)^2 + E^2 \Gamma_k^2} \quad (7)$$

in the last step [34–36]. The sum runs over the three axes of the nuclear quadrupoloid along which the GDR can oscillate with the SLO parameters E_{0k} , σ_{0k} and Γ_k ; i.e., the centroid energy, the peak photoabsorption cross section and the FWHM of the respective resonances. Naturally, the nuclear axes can be degenerate (axially-symmetric or spherical nuclei), making the SLO parameters possibly degenerate as well. For the cross section of SRS [67] of the GDR to the 2_1^+ state,

$$\sigma_{2_1^+}(E) = \frac{4\pi}{3} \sum_{k,l=1}^3 |f_{\text{GDR}_k}(E) - f_{\text{GDR}_l}(E)|^2 \quad (8)$$

is obtained [34, 35, 68] in the geometrical model of three orthogonal oscillators, where the $f_{\text{GDR}_k}(E)$ are the summands in Eq. (6). We stress that Eq. (8) assumes the 2_1^+ state to be the pure rotational excitation of the ground state. Furthermore, we note that the corresponding Alaga rule [69] for the $\sigma_{2_1^+}/\sigma_{\text{ES}}$ branching ratio is recovered from Eqs. (4) and (8) when an axially-symmetric nucleus with isolated $K = 0$ and $K = 1$ resonances, i.e. $\Gamma_K \ll |E_{K=1} - E_{K=0}|$, is considered and Thomson scattering is neglected. To test in detail this modelling of the GDR as an isovector oscillation of a quadrupoloid with respect to its three intrinsic major axes, a simultaneous Bayesian inference fit [57–60] was performed of the nine SLO parameters to both the new $\sigma_{2_1^+}/\sigma_{\text{ES}}$ γ -decay data and the existing σ_{abs} photoabsorption data [70] for ^{154}Sm . For comparison, a similar fit to only the prior known photoabsorption data was also carried out. The fits are shown in Fig. 2. While both can reproduce the photoabsorption data, and the ES cross section which was not fitted explicitly, fitting the SLO parameters only to the literature σ_{abs} photoabsorption cross section gives a non-satisfactory description of the $\sigma_{2_1^+}/\sigma_{\text{ES}}$ γ -decay data. A better description is obtained when also fitting to this data. This demonstrates the high sensitivity of the γ decay to small differences among the SLO parameters—details which cannot be obtained from the photoabsorption data alone. Note that this statement also holds when fitting an axially-symmetric nuclear shape instead with identical SLO parameters for the second and third GDR Lorentzians. Since the simultaneous fit can reproduce both datasets, σ_{abs} and $\sigma_{2_1^+}/\sigma_{\text{ES}}$, with high accuracy, the present data confirms the applicability of the geometrical model of the GDR even for its γ decay. The fitted SLO parameters are given in Table II.

Within the geometrical model, the resonance energy of a GDR oscillation is directly related to the length of the nuclear axes R_k along which it takes place [6, 28]; i.e.

$$E_{0k} \propto \frac{1}{R_k(\beta, \gamma)} \propto \frac{1}{1 + \sqrt{\frac{5}{4\pi}} \beta \cos[\gamma - \frac{2\pi}{3}(k-1)]} \quad (9)$$

where β and γ are the nuclear deformation parameters [71, 72]. Hence, the fit of Fig. 2 also yields infor-

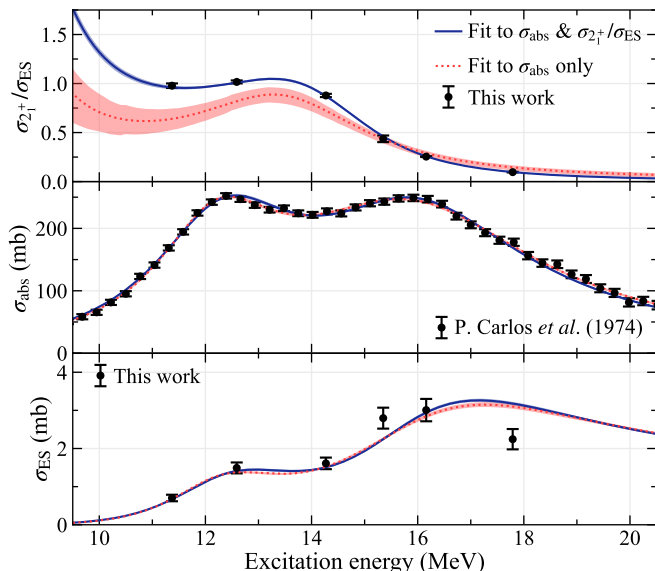


FIG. 2. Simultaneous fit (solid blue) of the SLO parameters of the ^{154}Sm GDR to both its $\sigma_{2^+}/\sigma_{\text{ES}}$ γ -decay behavior (top, data from this work) and its σ_{abs} photoabsorption cross section (middle, data from Ref. [70]) and fit (dotted red) just to the latter with 1-sigma uncertainty bands. Both fits describe the photoabsorption data well. The γ -decay branching ratio can only be reproduced when it is explicitly included in the fit, while the good description of the photoabsorption cross section is preserved. This demonstrates its high sensitivity to SLO parametrization—details which cannot be obtained from the photoabsorption data alone. The ES cross section (bottom, data from this work) is not explicitly fitted. Still, modelling the GDR as single resonances along the three axes accounts well for these data in both fits.

TABLE II. SLO parameters of the ^{154}Sm GDR obtained from the simultaneous fit to its $\sigma_{2^+}/\sigma_{\text{ES}}$ (this work) and σ_{abs} (Ref. [70]) datasets. See text for details.

k	E_{0k} (MeV)	Γ_k (MeV)	σ_{0k} (mb)
1	12.384(30)	3.305(84)	199.3(25)
2	15.905(74)	4.24(20)	108.9(60)
3	16.395(87)	5.95(32)	103.6(56)

mation on the nuclear shape of ^{154}Sm and, in particular, provides constraints on its nuclear triaxiality from the energy splitting of its second and third GDR Lorentzians. By reparametrizing the E_{0k} values in the fit through the nuclear deformation parameters according to Eq. (9), posterior distributions of the ^{154}Sm quadrupole deformation parameter β and its triaxiality angle γ are obtained through both fits. These can be found in Fig. 3. Fitting the previously known photoabsorption data only results in a rather flat, featureless posterior distribution for the γ deformation with a 99.7% credible upper limit of 23.3° . The fit performed while considering in addition the new γ -decay data, however, yields an almost

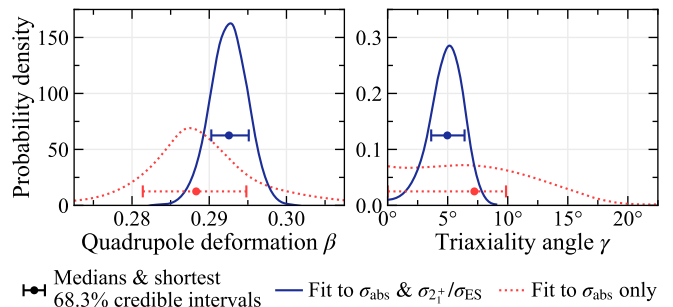


FIG. 3. Posterior distributions for the quadrupole deformation parameter β and the triaxiality angle γ of ^{154}Sm obtained from its fitted GDR resonance energies E_{0k} for both fits shown in Fig. 2. While fitting only the photoabsorption data results in a broad, featureless distribution for γ , considering also the γ -decay behavior yields a significantly more constrained, almost Gaussian distribution. Likewise, for β both posteriors agree overall, but considering the γ -decay behavior yields a more constrained distribution with a slightly shifted median. The uncertainty bars illustrate the medians and shortest 68.3% credible intervals of the respective posterior distributions.

Gaussian distribution centered around 5° with a significantly lower 99.7% credible upper limit of 8.3° . Similarly, for the β deformation, both posteriors agree overall, but taking into account the γ -decay behavior yields a more constrained distribution with a slightly shifted median. Taking the median and shortest 68.3% credible intervals, $\beta = 0.2926(26)$ and $\gamma = 5.0(14)^\circ$ are obtained from the simultaneous fit. These results match well with the most-recent state-of-the-art configuration interaction calculations in the Monte Carlo Shell Model, which predict $\beta \approx 0.28$ and $\gamma \approx 3.7^\circ$ for the ground-state deformation of ^{154}Sm [73, 74]. The present β value disagrees by 16% with the value $\beta_2 = 0.3404(17)$ obtained from the $B(E2; 0_1^+ \rightarrow 2_1^+) = 4.345(44) e^2 b^2$ ^{154}Sm transition strength in the compilation of Ref. [75]. However, this discrepancy originates from the sole usage of the leading order of the $B(E2)$ -to- β^2 relation and from assuming the solid-angle mean nuclear radius R_0 to be $1.2 \text{ fm} \cdot A^{1/3}$ without uncertainty. Using instead the full relation [76, 77]

$$B(E2; 0_1^+ \rightarrow 2_1^+) = \left[\frac{3}{4\pi} Z e R_0^2 \left(\beta + \frac{1}{8} \sqrt{\frac{5}{\pi}} \beta^2 \right) \right]^2 \quad (10)$$

and $R_0 = \sqrt{5/3} \sqrt{\langle r^2 \rangle}$ for the mean nuclear radius [78], with $\sqrt{\langle r^2 \rangle} = 5.126(8) \text{ fm}$ being the root-mean-square charge radius measured in elastic electron scattering on ^{154}Sm [79], $\beta = 0.3067(17)$ is obtained from the $B(E2; 0_1^+ \rightarrow 2_1^+)$ strength [75]. This β value agrees with the result of the GDR fit within 5%. Similarly [76, 77], $\beta = 0.304(6)$ is obtained from the spectroscopic quadrupole moment $Q(2_1^+) = -1.87(4) \text{ b}$ of the 2_1^+ state of ^{154}Sm of Ref. [48]. This in turn matches with the

TABLE III. ^{154}Sm Deformation parameters β and γ obtained from different approaches and observables. See text for details.

Approach/Observables	β	γ ($^\circ$)
GDR σ_{abs} [70] and $\sigma_{2^+}/\sigma_{\text{ES}}$ (this work)	0.2926(26)	5.0(14)
$B(E2; 0_1^+ \rightarrow 2_1^+)$ [75] and $\sqrt{\langle R_0^2 \rangle}$ [79]	0.3067(17)	
$B(E2; 0_1^+ \rightarrow 2_1^+)$ leading order only [75]	0.3404(17)	
$Q(2_1^+)$ [48] and $\sqrt{\langle R_0^2 \rangle}$ [79]	0.304(6)	
Monte Carlo Shell Model [73, 74]	≈ 0.28	≈ 3.7

result of the GDR fit. Table III compares the deformation parameters obtained from the different observables and approaches. The remaining small discrepancy may be due to some of the assumptions in the various approaches not being entirely fulfilled. For example, ^{154}Sm may not be exactly rigid, as inferred from, e.g., the confined β -soft rotor model [80, 81], where, due to the finite width of the potential well in β , the wave functions extracted from $E2$ properties have fluctuations. The latter result in larger $E2$ matrix elements and, hence, larger effective β values than under a rigid rotor assumption. In addition, due to pairing, the physical ground state might be energetically lower than assumed in the geometrical model of the GDR. This would result in an underestimation of β in the GDR fit. It should be emphasized, that the latter would not have a significant effect on the determination of the triaxiality. Considering the overall good agreement of the β deformation parameters obtained from the $B(E2; 0_1^+ \rightarrow 2_1^+)$ strength, the $Q(2_1^+)$ moment and the GDR γ decay, the high sensitivity of the latter to the nuclear shape is validated. In particular, a noteworthy sensitivity to the triaxiality degree of freedom is achieved, with a small value of $\gamma = 5.0(14)^\circ$ for ^{154}Sm . This finding contributes to the contemporary debate on nuclear triaxial shapes [72, 74, 82–87].

While this is the first measurement of the evolution of the 2_1^+ -SRS to ES branching ratio of the GDR for a deformed nucleus as a function of energy, it is of interest to investigate this quantity in other nuclei such as ^{166}Er [74], ^{164}Dy [73] and ^{188}Os [88], where triaxialities $\gamma > 7^\circ$ are predicted. Likewise, the γ -decay behavior of the GDRs of ^{152}Sm and ^{150}Nd would merit further experiments due to proximity of these nuclei to the spherical-to-deformed shape phase transition [89–91], which is expected to be accompanied by an increased softness in β deformation. The GDR's photoabsorption data for these nuclei and, therefore, the splitting of their GDRs have been disputed recently [92]. The γ decay of the GDR is a yet untapped observable highly sensitive both to the structure of the GDR and to the nuclear ground state from which it is photoexcited. Thus, new measurements would provide further insights in these cases. Moreover, measurement of the γ decay of the GDR in spherical nuclei will constrain state-of-the-art nuclear theory [93].

In summary, NRF experiments on the GDR of the deformed nucleus ^{154}Sm were performed at HI γ S to study the properties associated with its γ decay. The measured $\sigma_{2^+}/\sigma_{\text{ES}}$ ratios are described well with the macroscopic model of the GDR. This result validates the power of this model and establishes γ decay as a novel observable sensitive to the structure of the GDR. Further investigations with this technique have the potential of providing constraints on nuclear shape parameters, especially on the triaxiality parameter, for nuclei throughout the nuclear chart. They can also provide further insights in instances where the structure of the GDR itself is controversial [92].

The full data and analysis underlying this letter are openly available at the TUdataLib repository of Technische Universität Darmstadt [94] and further details will soon be available in Ref. [95].

We thank the HI γ S accelerator group for providing perfect conditions for our experiments and L. Fortunato, H.-W. Hammer and T. Otsuka for valuable discussions. This work has been funded by the German state of Hesse's Ministry of Higher Education, Research and the Arts (HMWK) under grant No. LOEWE/2/11/519/03/04.001(0008)/62, by the Deutsche Forschungsgemeinschaft (DFG, German Research Foundation) – Project-ID 499256822 – GRK 2891, by the German Federal Ministry of Education and Research (BMBF) under grant No. 05P21RDEN9, and by the U.S. Department of Energy, Office of Nuclear Physics, under grant Nos. DE-FG02-97ER41041 (UNC) and DE-FG02-97ER41033 (TUNL/Duke).

* jkleemann@ikp.tu-darmstadt.de

† Present address: Vysus Group Sweden AB, 214 21 Malmö, Sweden

‡ Present address: Facility for Rare Isotope Beams, Michigan State University, East Lansing, Michigan 48824, USA

- [1] B. L. Berman and S. C. Fultz, *Rev. Mod. Phys.* **47**, 713 (1975).
- [2] N. Otsuka *et al.*, *Nucl. Data Sheets* **120**, 272 (2014).
- [3] M. N. Harakeh and A. Van der Woude, *Giant Resonances: Fundamental High-Frequency Modes of Nuclear Excitation*, Oxford Studies in Nuclear Physics, Vol. 24 (Oxford University Press, 2001).
- [4] W. Kuhn, *Z. Phys.* **33**, 408 (1925).
- [5] F. Reiche and W. Thomas, *Z. Phys.* **34**, 510 (1925).
- [6] J. Speth and A. van der Woude, *Rep. Prog. Phys.* **44**, 719 (1981).
- [7] W. Bothe and W. Gentner, *Z. Phys.* **106**, 236 (1937).
- [8] G. C. Baldwin and G. S. Klaiber, *Phys. Rev.* **71**, 3 (1947).
- [9] G. C. Baldwin and G. S. Klaiber, *Phys. Rev.* **73**, 1156 (1948).
- [10] P. F. Bortignon, A. Bracco, and R. A. Broglia, *Giant Resonances: Nuclear Structure at Finite Temperature* (Harwood Academic Publishers, 1998).
- [11] S. Goriely, P. Dimitriou, M. Wiedeking, T. Belgia,

- R. Firestone, J. Kopecky, M. Krťicka, V. Plujko, R. Schwengner, S. Siem, H. Utsunomiya, S. Hilaire, S. Péru, Y. S. Cho, D. M. Filipescu, N. Iwamoto, T. Kawano, V. Varlamov, and R. Xu, *Eur. Phys. J. A* **55**, 172 (2019).
- [12] A. Bracco, F. Camera, F. C. L. Crespi, B. Million, and O. Wieland, *Eur. Phys. J. A* **55**, 233 (2019).
- [13] O. Wieland, A. Bracco, F. Camera, G. Benzoni, N. Blasi, S. Brambilla, F. Crespi, A. Giussani, S. Leoni, P. Mason, B. Million, A. Moroni, S. Barlini, V. L. Kravchuk, F. Gramegna, A. Lanchais, P. Mastinu, A. Maj, M. Brekiesz, M. Kmiecik, M. Bruno, E. Geraci, G. Vannini, G. Casini, M. Chiari, A. Nannini, A. Ordine, and E. Ormand, *Phys. Rev. Lett.* **97**, 012501 (2006).
- [14] M. P. Kelly, K. A. Snover, J. P. S. van Schagen, M. Kicińska-Habior, and Z. Trznadel, *Phys. Rev. Lett.* **82**, 3404 (1999).
- [15] A. Bracco, F. Camera, M. Mattiuzzi, B. Million, M. Pignanelli, J. J. Gaardhøje, A. Maj, T. Ramsøy, T. Tveter, and Z. Żelazny, *Phys. Rev. Lett.* **74**, 3748 (1995).
- [16] D. L. Ederer, *Phys. Rev. Lett.* **13**, 760 (1964).
- [17] A. P. Lukirskii, I. A. Brytov, and T. M. Zimkina, *Opt. Spektrosk.* **17**, 234 (1964).
- [18] J. A. R. Samson (Academic Press, 1966) pp. 177–261.
- [19] G. Wendin, *Phys. Lett. A* **46**, 119 (1973).
- [20] A. D. Shiner, B. E. Schmidt, C. Trallero-Herrero, H. J. Wörner, S. Patchkovskii, P. B. Corkum, J.-C. Kieffer, F. Légaré, and D. M. Villeneuve, *Nat. Phys.* **7**, 464 (2011).
- [21] S. Pabst and R. Santra, *Phys. Rev. Lett.* **111**, 233005 (2013).
- [22] W. A. de Heer, K. Selby, V. Kresin, J. Masui, M. Vollmer, A. Chatelain, and W. D. Knight, *Phys. Rev. Lett.* **59**, 1805 (1987).
- [23] W. Hoheisel, K. Jungmann, M. Vollmer, R. Weidenauer, and F. Träger, *Phys. Rev. Lett.* **60**, 1649 (1988).
- [24] J. Tiggesbäumker, L. Köller, H. O. Lutz, and K. H. Meives-Broer, *Chem. Phys. Lett.* **190**, 42 (1992).
- [25] G. Gensterblum, J. J. Pireaux, P. A. Thiry, R. Caudano, J. P. Vigneron, P. Lambin, A. A. Lucas, and W. Krätschmer, *Phys. Rev. Lett.* **67**, 2171 (1991).
- [26] I. V. Hertel, H. Steger, J. de Vries, B. Weissner, C. Menzel, B. Kamke, and W. Kamke, *Phys. Rev. Lett.* **68**, 784 (1992).
- [27] M. Goldhaber and E. Teller, *Phys. Rev.* **74**, 1046 (1948).
- [28] H. Steinwedel and J. H. D. Jensen, *Z. Naturforsch. A* **5**, 413 (1950).
- [29] J. Speth and J. Wambach, Theory of giant resonances, in *Electric and Magnetic Giant Resonances in Nuclei*, International Review of Nuclear Physics, Vol. 7, edited by J. Speth (World Scientific Publishing Company, 1991) pp. 1–97.
- [30] J. R. Beene *et al.*, *Phys. Rev. C* **41**, 920 (1990).
- [31] K. Boretzky *et al.*, *Phys. Lett. B* **384**, 30 (1996).
- [32] M. Danos, *Nucl. Phys.* **5**, 23 (1958).
- [33] K. Okamoto, *Phys. Rev.* **110**, 143 (1958).
- [34] E. Hayward, *Photonuclear Reactions*, NBS monograph (U.S. National Bureau of Standards, Gaithersburg, MD, 1970).
- [35] E. G. Fuller and E. Hayward, *Nucl. Phys.* **30**, 613 (1962).
- [36] T. Bar-Noy and R. Moreh, *Nucl. Phys. A* **229**, 417 (1974).
- [37] H. E. Jackson, G. E. Thomas, and K. J. Wetzel, *Phys. Rev. C* **11**, 1664 (1975).
- [38] A. M. Nathan and R. Moreh, *Phys. Lett. B* **91**, 38 (1980).
- [39] A. M. Nathan, *Phys. Rev. C* **38**, 92 (1988).
- [40] S. D. Hoblit and A. M. Nathan, *Phys. Rev. C* **44**, 2372 (1991).
- [41] A. Zilges, D. L. Balabanski, J. Isaak, and N. Pietralla, *Prog. Part. Nucl. Phys.* **122**, 103903 (2022).
- [42] U. Kneissl, H. H. Pitz, and A. Zilges, *Prog. Part. Nucl. Phys.* **37**, 349 (1996).
- [43] U. Kneissl, N. Pietralla, and A. Zilges, *J. Phys. G: Nucl. Part. Phys.* **32**, R217 (2006).
- [44] J. Isaak and N. Pietralla, Probing nuclear structure with photon beams, in *Handbook of Nuclear Physics*, edited by I. Tanihata, H. Toki, and T. Kajino (Springer Nature Singapore, Singapore, 2022) pp. 1–45.
- [45] H. R. Weller, M. W. Ahmed, H. Gao, W. Tornow, Y. K. Wu, M. Gai, and R. Miskimen, *Prog. Part. Nucl. Phys.* **62**, 257 (2009).
- [46] H. R. Weller, M. W. Ahmed, and Y. K. Wu, *Nucl. Phys. News* **25**, 19 (2015).
- [47] A. D. Ayangeakaa, U. Friman-Gayer, and R. V. F. Janssens, *Innovation News Network* (2021).
- [48] C. W. Reich, *Nucl. Data Sheets* **110**, 2257 (2009).
- [49] R. M. Steffen and K. Alder, in *The Electromagnetic Interaction in Nuclear Spectroscopy*, edited by W. D. Hamilton (North-Holland, Amsterdam, NL, 1975) Chap. 12, pp. 505–582.
- [50] K. S. Krane, R. M. Steffen, and R. M. Wheeler, *At. Data Nucl. Data Tables* **11**, 351 (1973).
- [51] L. W. Fagg and S. S. Hanna, *Rev. Mod. Phys.* **31**, 711 (1959).
- [52] C. Iliadis and U. Friman-Gayer, *Eur. Phys. J. A* **57**, 190 (2021).
- [53] S. Agostinelli *et al.* (GEANT4 collaboration), *Nucl. Instrum. Methods Phys. Res. A* **506**, 250 (2003).
- [54] J. Allison *et al.* (GEANT4 collaboration), *IEEE Trans. Nucl. Sci.* **53**, 270 (2006).
- [55] J. Allison *et al.* (GEANT4 collaboration), *Nucl. Instrum. Methods Phys. Res. A* **835**, 186 (2016).
- [56] U. Friman-Gayer, J. Kleemann, and O. Papst, *u-eff-gee/utr: GEANT4 simulation of the Upper Target Room (UTR) at the HIGS facility v2024.01* (2024).
- [57] A. Gelman, J. B. Carlin, H. S. Stern, and D. B. Rubin, *Bayesian data analysis*, 3rd ed. (Chapman & Hall/CRC, 2014).
- [58] S. Brooks, A. Gelman, G. Jones, and X.-L. Meng, *Handbook of Markov Chain Monte Carlo* (Chapman and Hall/CRC, 2011).
- [59] J. Salvatier, T. V. Wiecki, and C. Fonnesbeck, *PeerJ Comput. Sci.* **2**, e55 (2016).
- [60] T. Wiecki *et al.*, *pymc-devs/pymc: Bayesian modeling and probabilistic programming in python v5.10.3* (2023).
- [61] J. Kelley, J. E. Purcell, and C. G. Sheu, *Nucl. Phys. A* **968**, 71 (2017).
- [62] M. Shamsuzzoha Basunia, *Nucl. Data Sheets* **114**, 1189 (2013).
- [63] N. Nica, *Nucl. Data Sheets* **154**, 1 (2018).
- [64] S. C. Fultz, R. L. Bramblett, J. T. Caldwell, and N. A. Kerr, *Phys. Rev.* **127**, 1273 (1962).
- [65] A. Leprêtre, H. Beil, R. Bergère, P. Carlos, J. Fagot, A. D. Miniac, A. Veyssiére, and H. Miyase, *Nucl. Phys. A* **258**, 350 (1976).
- [66] D. Drechsel, B. Pasquini, and M. Vanderhaeghen, *Phys. Rep.* **378**, 99 (2003).
- [67] S. Bhagavantam, *Scattering of light and the Raman effect*

- (Chemical Publishing Company, Inc., 1942).
- [68] Z. Marić and P. Möbius, *Nucl. Phys.* **10**, 135 (1959).
 - [69] G. Alaga, K. Alder, A. Bohr, and B. R. Mottelson, *Dan. Mat. Fys. Medd.* **29**, 1 (1955).
 - [70] P. Carlos, H. Beil, R. Bergère, A. Leprêtre, A. D. Miniac, and A. Veyssiére, *Nucl. Phys. A* **225**, 171 (1974).
 - [71] A. Bohr and B. R. Mottelson, *Nuclear Structure Volume II* (W.A. Benjamin, Inc., 1975).
 - [72] A. S. Davydov and G. F. Filippov, *Nucl. Phys.* **8**, 237 (1958).
 - [73] T. Otsuka, Y. Tsunoda, N. Shimizu, Y. Utsuno, T. Abe, and H. Ueno (2024), in preparation.
 - [74] T. Otsuka, Y. Tsunoda, T. Abe, N. Shimizu, and P. Van Duppen, *Phys. Rev. Lett.* **123**, 222502 (2019).
 - [75] B. Pritychenko, M. Birch, B. Singh, and M. Horoi, *At. Data Nucl. Data Tables* **107**, 1 (2016).
 - [76] K. E. G. Löbner, M. Vetter, and V. Hönl, *At. Data and Nucl. Data Tables* **7**, 495 (1970).
 - [77] R. F. Casten, *Nuclear Structure from a Simple Perspective*, 2nd ed. (Oxford University Press, 2000).
 - [78] K. S. Krane, *Introductory Nuclear Physics*, 3rd ed. (John Wiley & Sons, 1987).
 - [79] H. De Vries, C. W. De Jager, and C. De Vries, *At. Data Nucl. Data Tables* **36**, 495 (1987).
 - [80] N. Pietralla and O. M. Gorbachenko, *Phys. Rev. C* **70**, 011304(R) (2004).
 - [81] T. Möller *et al.*, *Phys. Rev. C* **86**, 031305(R) (2012).
 - [82] E. Grosse, A. R. Junghans, and R. Massarczyk, *Eur. Phys. J. A* **53**, 225 (2017).
 - [83] E. Grosse, A. R. Junghans, and J. N. Wilson, *Phys. Scr.* **92**, 114003 (2017).
 - [84] M. Lettmann *et al.*, *Phys. Rev. C* **96**, 011301(R) (2017).
 - [85] Y. Toh *et al.*, *Phys. Rev. C* **87**, 041304(R) (2013).
 - [86] L. Guo, J. A. Maruhn, and P.-G. Reinhard, *Phys. Rev. C* **76**, 034317 (2007).
 - [87] A. D. Ayangeakaa *et al.*, *Phys. Rev. C* **107**, 044314 (2023).
 - [88] A. Hayashi, K. Hara, and P. Ring, *Phys. Rev. Lett.* **53**, 337 (1984).
 - [89] F. Iachello, *Phys. Rev. Lett.* **87**, 052502 (2001).
 - [90] R. F. Casten and N. V. Zamfir, *Phys. Rev. Lett.* **87**, 052503 (2001).
 - [91] R. Krücken *et al.*, *Phys. Rev. Lett.* **88**, 232501 (2002).
 - [92] L. M. Donaldson *et al.*, *Phys. Lett. B* **776**, 133 (2018).
 - [93] W. L. Lv, Y. F. Niu, and G. Colò, *Phys. Rev. C* **103**, 064321 (2021).
 - [94] J. Kleemann *et al.*, Dataset and analysis codes for "Gamma decay of the ^{154}Sm isovector giant dipole resonance: Smekal-raman scattering as a novel probe of nuclear ground-state deformation", TUDatalib, Technische Universität Darmstadt (2024).
 - [95] J. Kleemann, *Dissertation*, Technische Universität Darmstadt, Darmstadt, in preparation.